

Formation of Mixed Binary Clusters in a Supersonic Molecular Beam: A Nice Case of RRK Kinetics

Bernd R. Veenstra, Harry T. Jonkman, and Jan Kommandeur*

Laboratory for Chemical Physics, Materials Science Center, University of Groningen, Nijenborgh 4, 9747 AG Groningen, The Netherlands

Received: October 18, 1993; In Final Form: November 4, 1993*

A kinetic model is presented which explains the nonstatistical cluster distributions found in a supersonic expansion of binary mixtures of weakly interacting organic molecules. It is shown that clustering in a supersonic expansion leads to a fractionation of the clusters, i.e., to an enrichment of the most strongly bound component. In our model we consider in the step-by-step growing process of the cluster three important events. In a first step the cluster grows by the addition of a monomer and forms an activated complex. This complex can be stabilized by a collision with an atom of the monatomic carrier gas, or it can be stabilized by a branching process in which it loses the same type of monomer or by a substitution process in which the other type of molecule is leaving. As follows from the RRK equations, for the addition of the strongly bound component the substitution reaction rate is much faster than for the addition of the more weakly bound component. This gives rise to the nonstatistical enrichment toward the more strongly bound species as observed. For comparison with our experimental results, it is important to include the physics of the supersonic expansion process in our model calculation, because it is essential that the clustering process freezes in at an early stage. We show that the experimental results can be accounted for with our kinetic model with only two parameters: the stabilization efficiency of the monatomic carrier gas and the average temperature of the clusters.

Introduction

In an earlier paper¹ we reported on the formation of mixed clusters of organic molecules in a supersonic beam. It was already noticed then that in general the composition of the clusters did not reflect the composition of the vapor phase from which they were formed. Instead, they were highly enriched toward the side of the most strongly bound molecule. For instance, a mixture of benzene and cyclohexane was strongly enriched on the benzene side. Apparently, the higher polarizability of benzene, due to the π -electrons, leads to stronger bonding of this molecule. Similarly, heptane dominated in hexane/heptane clusters simply because of the larger size and therefore the larger polarizability of the heptane molecule.

At the time of our previous paper it was not at all clear what the enrichment was due to. Was it due to the kinetics of the formation, or was it due to the ionization and the subsequent preferential boil-off of the more weakly bound component? Indeed, the measurements as a function of the electron energy for ionization appeared to point toward the boil-off mechanism. However, since then, measurements by Schlag and co-workers² and Booze and Baer³ have shown quite clearly that the overriding event after ionization is the loss of one molecule. Ernstberger et al.⁴ demonstrated that mixed clusters of benzene and toluene lose only one monomer in metastable fragmentation: the weakest bound component. This is by no means sufficient to explain the strong enrichment that takes place: the enrichment must come about during the formation stage of the clusters.

We therefore decided to study the intensity distributions in various small binary clusters more quantitatively under closely controlled conditions. We basically found the results we had observed earlier, be it that we had much better quantitative data. For the explanation of the strong enrichment of the small clusters, neither the classical nucleation theory⁵ nor the revised classical theory of Wilemski⁶ for binary mixtures is suitable, because both theories heavily rely on the description of microscopic cluster phenomena with macroscopic parameters and both theories consider clusters as spherical droplets. The latter assumption

will be correct for large clusters where shell closings have taken place but is doubtful for the cluster sizes we study. Also, the nonclassical model of Zeng and Oxtoby⁷ for binary clusters, although starting from microscopic intermolecular parameters, describes nucleation of larger droplets.

For the formation of a small cluster it is important to realize that a cluster is formed as a collision complex containing excess energy. The cluster can dispose of this energy by collision with a carrier gas atom or by the loss of a monomer. If a strongly bound molecule is attached to a mixed cluster, the resulting complex can either dissociate by the loss of a strongly bound species or lose a more weakly bound molecule in a substitution reaction. The reverse substitution reaction, a weakly bound molecule replacing a more strongly bound one, is not allowed if the cluster is completely cold. However, if the cluster contains some energy, this reaction also becomes possible, but will have a very low rate. Then it is the difference between the two substitution reaction rates that leads to the observed enrichment of small clusters. We can only observe the enrichment in a supersonic expansion, where cluster distributions are frozen in at an early stage of the formation process.

After a short experimental part, we discuss the kinetic equations, the modeling of the supersonic expansion, and then the results and their interpretation. It will turn out that the dimer formation is the critical step in the kinetic process, so it is discussed more extensively. The rate constants involved in the formation of larger clusters are described in terms of RRK theory.⁸ A remarkably consistent picture emerges.

Experimental Section

The supersonic beam apparatus was very similar to the one described before.¹ Since our mass spectrometer measured masses up to 1000 amu, we concentrated on the smaller clusters and therefore used a flat instead of a conical nozzle.

The clustering mixtures were benzene/toluene and toluene/*o*-xylene. For the benzene/toluene mixture, the vapor pressure as a function of composition of the liquid is very well known.⁹ The toluene/*o*-xylene phase diagram we measured ourselves. The

* Abstract published in *Advance ACS Abstracts*, March 1, 1994.

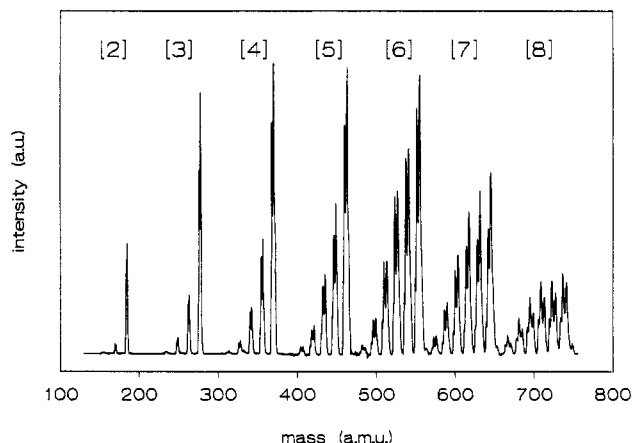


Figure 1. Experimental cluster mass spectrum of clusters 2–8 of a 70:30 vapor mixture of benzene/toluene. The spectrum was recorded at an ionization energy of 13.5 eV. Every group of cluster peaks with the same number of constituents was recorded separately with a different resolution. The intensity distribution in the cluster peaks is far from that given by the relative concentrations.

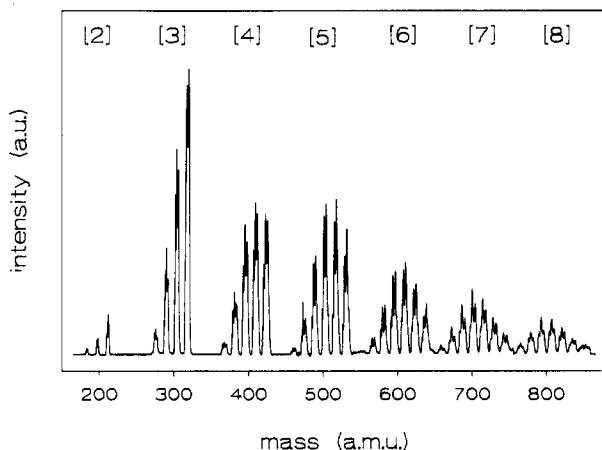


Figure 2. Experimental cluster mass spectrum of a 70:30 vapor mixture of toluene/o-xylene. The intensity distribution is less enriched than in the benzene/toluene cluster spectrum.

mixtures required were made up volumetrically and equilibrated at room temperature. The vapor was first leaked into the mass spectrometer, together with about 1.5 bar of He, and the intensities of the peaks of the pure monomers were measured. In both mixtures the intensities turned out to be a linear function of the corresponding liquid mole fraction. Together with the vapor pressures of the pure compounds¹⁰ they gave the composition of the vapor phase.

We then flowed the vapor mixture into the nozzle. The resulting clusters, after having passed a 0.7-mm skimmer and a 1-mm consecutive skimmer, were observed about 80 cm downstream. To ensure the least possible decomposition after ionization, the mass spectra were recorded at the very low electron energy of 13.5 eV. The quadrupole mass spectrometer signal was read into a computer, which allowed further processing of the data. Typical results for both mixtures are shown in Figures 1 and 2. The spectra are highly enriched in the heavier components, i.e., toluene in Figure 1 and o-xylene in Figure 2.

Kinetic Equations

We consider a mixture of molecules A and B, where B is the one with the strongest binding to itself and to A.

The first step in cluster growth is of course the formation of the dimer, the formation of a trimer in a three-body collisions being too unlikely in the dilute systems we consider. The van der Waals condensation energy will be dumped into the bond joining

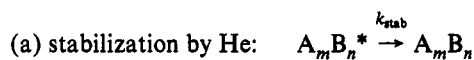
the two molecules. In general, this bond will not couple strongly to the internal vibrations of the molecule, so if the energy is not carried off during the collision, the collision complex will dissociate again.

The dimer formation needs mediation by a third body, i.e., a helium atom in the expansions considered. We will further discuss the efficiency of such dimer–helium collisions below, suffice it to say here that the efficiency of dimer formation will be small. Most encounters of monomers will be unsuccessful.

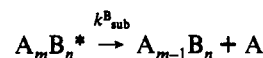
Further growth of the cluster mainly involves cluster–monomer collisions in our dilute system. This growth is easier than dimer formation, since there are more modes into which the “condensation” energy can be temporarily stored. Nevertheless, most attempts at clustering by collisions will still fail. Kinetically, we can describe this process with the following equations, where $A_mB_n^*$ denotes an “activated complex”, a collision complex which has not yet disposed of its energy. For the collision of a cluster with B we have

$$d[A_mB_n^*]/dt = k_f^B[A_mB_{n-1}][B]$$

with the rate constant $k_f^B = (8k_B T_L / \pi \mu)^{1/2} \sigma(m, n)$, where k_B is the Boltzmann constant, T_L the local temperature, μ the reduced mass of cluster and monomer, and $\sigma(m, n)$ the collision cross section of cluster and monomer. The activated complex $A_mB_n^*$ has three routes to lose its energy:



and since the binding energy of B is higher than that of A:

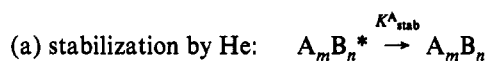


Here the stabilization rate constant $k_{stab} = \xi n_{He} \sigma(m, n, He) (8k_B T_L / \pi m_{He})^{1/2}$ with ξ the efficiency of a helium collision, n_{He} the density of helium, and m_{He} the mass of helium.

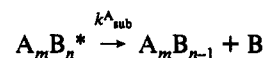
Similarly for the collision of a cluster with A

$$d[A_mB_n^*]/dt = k_f^A[A_{m-1}B][A]$$

with k_f^A having the same definition as above. For the deactivation we now have



Only when the cluster contains sufficient energy we have



since the binding energy of A by itself is not enough to dislodge B. The fact that this channel has a small rate constant is the reason for the enrichment of the clusters. The kinetic scheme has been depicted in Figure 3. The substitution will proceed as long as the kinetics runs, but finally it will so far exhaust B in preference to A that the A addition will start to become significant.

If we simulate cluster formation with the above reaction scheme and if we want to compare to our experiments, it is important to know the magnitude of the respective reaction rate constants. Also, we will have to “stop the kinetics” long before the A addition starts to dominate. In our experimental situation the kinetics

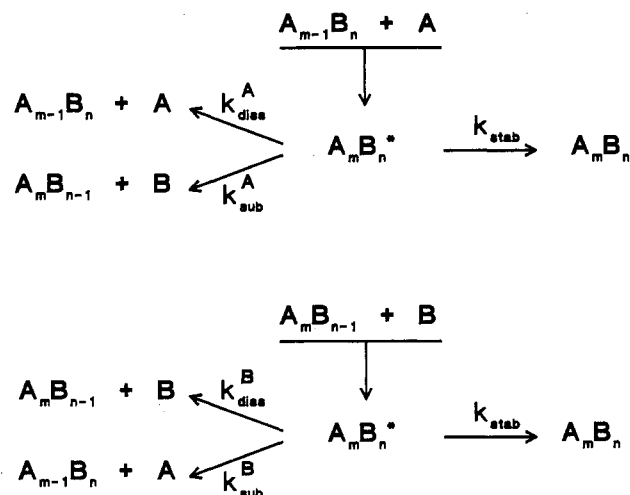


Figure 3. Kinetic scheme that leads to the enrichment of clusters in the most strongly bound component, B. Addition of A or B to the cluster releases energy. It takes less energy to lose A than to lose B; i.e., A will be lost more often and the cluster is enriched in B.

stop themselves, because there are no more collisions. We have to model the supersonic nozzle!

Modeling the Supersonic Nozzle

Following Habets¹¹ and Miller,¹² we assume that the expansion proceeds "in equilibrium", i.e., that collisions are so frequent that all information is exchanged. The state of the system is then completely determined by thermodynamic parameters, such as the local density n , the local pressure p , and the local temperature T . We do not consider any effects of thermal conductivity or viscosity, and we view the mixtures as ideal gases.

If u is the flow velocity and A the cross section of the flow, nAu = constant is the continuity equation. Further, if h is the enthalpy content per molecule and m the mass per molecule, we have

$$\frac{1}{2}mu^2 + h = h_0 \quad (1)$$

because the enthalpy is converted into kinetic energy of forward motion. The index 0 refers to stagnation conditions upstream from the nozzle where $u = 0$. With all initial enthalpy (h_0) converted this gives us the limiting value of u :

$$u_\infty = (2h_0/m)^{1/2} \quad (2)$$

Since we consider an ideal gas, we have

$$h = \gamma/(\gamma - 1)k_B T \quad (3)$$

in which γ is the specific heat ratio ($=5/3$ for monatomic gases) and k_B is the Boltzmann constant. This gives us

$$u_\infty = (\gamma/(\gamma - 1))^{1/2}(2k_B T_0/m)^{1/2} \quad (4)$$

with T_0 the temperature before the expansion. It now simply follows from (1) and (3)

$$\frac{T}{T_0} = \frac{h}{h_0} = 1 - \left(\frac{u}{u_\infty}\right)^2 \quad (5)$$

for the temperature, and for an adiabatic expansion we have

$$\frac{n}{n_0} = \left(\frac{T}{T_0}\right)^{(\gamma-1)^{-1}} = \left[1 - \left(\frac{u}{u_\infty}\right)^2\right]^{(\gamma-1)^{-1}} \quad (6)$$

To obtain the temperature and the density of the expanding gas anywhere along z , the forward direction, we need the velocity u as a function of z . Combining eqs 1 and 3, we obtain

$$\frac{u}{u_\infty} = \left(\frac{\gamma-1}{2}\right)^{1/2} M \left(1 + \frac{\gamma-1}{2} M^2\right)^{-1/2}$$

where the Mach number is defined as $M = u/a$, the ratio of the flow velocity u and the local speed of sound $a = (\gamma k_B T/m)^{1/2}$. Using the parameters given by Miller¹² for M as a function of z , we can calculate u , n , and T anywhere along the axis of the expansion.

The kinetics are calculated in the following manner:

We start at the nozzle exit and follow the expansion by taking successive time steps Δt . In every time step we calculate collision densities and hence the number of clusters formed. We assume that the heat of condensation, released upon clustering, is rapidly removed by helium and does not heat up the beam appreciably. We continue the calculation until the beam reaches the sudden freeze plane, where the collision free zone starts. For a 100- μ m nozzle with a He pressure of 1.5 atm, the location of the sudden freeze plane is given by $z_F = 1.2$ mm.¹¹

Finally, after the collision-free zone has been reached, we simulate the loss at ionization by removing one molecule from the cluster:²⁻⁴ the least polarizable one if that is possible, if not (as for a pure B cluster) the more polarizable one. The resulting computer generated intensities are compared to experiment.

Enrichment Due to Mass Only

It is well-known¹³⁻¹⁷ that supersonic beams tend to concentrate heavy masses in the center of the beam. This is due to two effects: pressure diffusion¹⁴⁻¹⁶ in the first three nozzle diameters downstream from the nozzle and Mach number focusing^{16,17} downstream from the sudden freeze plane.

In the first three nozzle diameters, streamlines are curved and large pressure and temperature gradients exist perpendicular to the streamlines, causing lighter particles to escape more easily from the beam axis than heavier particles. Rothe¹⁵ and Knuth¹⁶ give an expression for pressure diffusion, which is evaluated for $\gamma = 5/3$. The thermal diffusion ratio is taken from Landolt and Börnstein:¹⁸ $\alpha_0 = 0.9(m_H - m_L)/(m_H + m_L)$, where the indices H and L refer to the heavy and light species.

Once the beam reaches the collision-free zone, the perpendicular temperature still decreases, and therefore the beam is more rapidly diluted in the lighter species. This effect, Mach number focusing, is calculated according to Knuth:^{16,17}

$$\frac{(n_H/n_L)_d}{(n_H/n_L)_{z_F}} = \left(\frac{m_H}{m_L}\right)^{0.2} \left(\frac{2m_H}{m_H + m_L}\right)^{1.2} \left(\frac{\sigma_{HL}}{\sigma_{LL}}\right)^{1.6}$$

Here the index d refers to the concentration ratio at the detector; σ is the collision cross section.

We can include the effects of pressure diffusion and Mach number focusing in the equations of the supersonic expansion and calculate cluster formation.

Such calculations were performed, and they turned out to yield much less enrichment than necessary to explain our experiments. But to show the magnitude of the effect experimentally, we made mixed clusters of benzene and hexadeuterated benzene. The result is shown in Figure 4. It will be clear that the enrichment is much less than in the mass spectra of molecules which differ in their interaction. The cluster mass spectrum also serves as a calibration of our beam calculation. The calculated and observed enrichment are close.

Dimer Efficiency

As we pointed out above, most monomer-monomer collisions will not be successful, unless a He atom happens to be present. But even then, the dimer will only be stabilized if a sufficient amount of the sum of binding and kinetic energy (from the relative motions of the monomers) is carried off. If an elastic collision

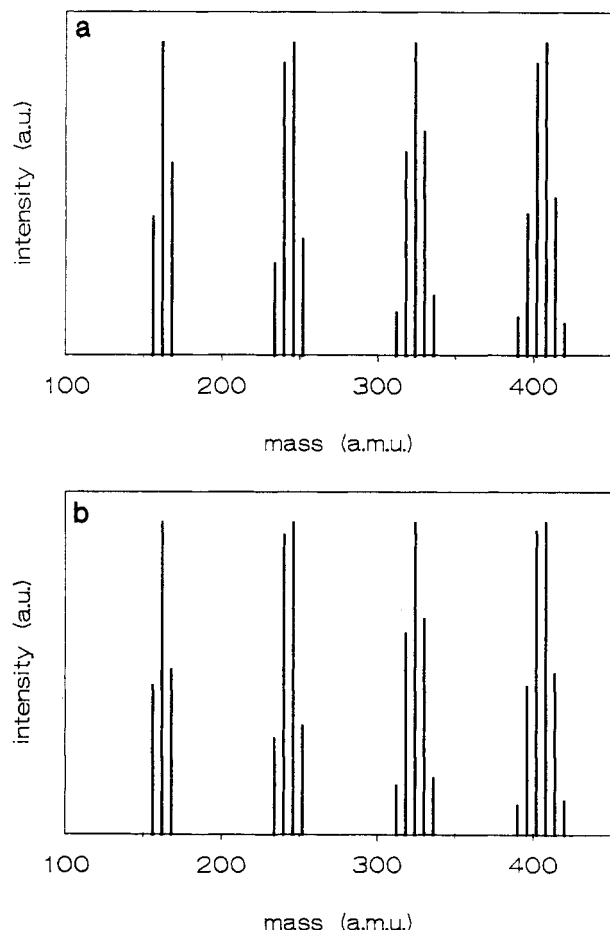


Figure 4. (a) Experimental cluster mass spectrum of a 50:50 vapor mixture of benzene/hexadeuterated benzene seeded into 2.5 atm of He. The spectrum was recorded at an ionization energy of 50 eV to obtain a large signal-to-noise ratio. Peaks are integrated for clarity. (b) Calculated cluster mass spectrum of a 50:50 vapor mixture of benzene/hexadeuterated benzene, using the equations described in the text. Corresponding experimental and calculated intensities agree within the error limits.

takes place, or if He adds energy to the monomers trying to form the dimer, a dissociation will ensue.

If all collisions are stochastically independent, the probability that an activated complex A_2^* has not collided with a He atom within its lifetime τ is given by¹⁹ $\exp(-\lambda\tau)$ with $\lambda = z_{He}$, the collision frequency of the dimer with helium. Hence, the probability that the complex has at least collided once with a He atom within its lifetime is given by

$$P(\tau) = 1 - \exp(-\tau z_{He}) \quad (7)$$

But if we consider only stabilizing collisions, we should use for z_{He} the effective collision number with He, which will be considerably smaller.

We have endeavored to estimate the fraction of successful He collisions by a molecular dynamics calculation. We first estimate the lifetime of the activated complex. In addition to the Lennard-Jones potential

$$V_{LJ}(r) = 4\epsilon \left[\left(\frac{\sigma}{r} \right)^{12} - \left(\frac{\sigma}{r} \right)^6 \right]$$

we have to take into account the centrifugal barrier arising for non-head-on collisions. The lifetime τ_{coll} in the collision was calculated by Bunker²⁰ and is

$$\tau_{coll} = 1.50\sigma\mu^{1/2}\epsilon^{1/6}E_0^{-2/3}$$

where σ , ϵ , and μ have their usual meaning as in the LJ potential

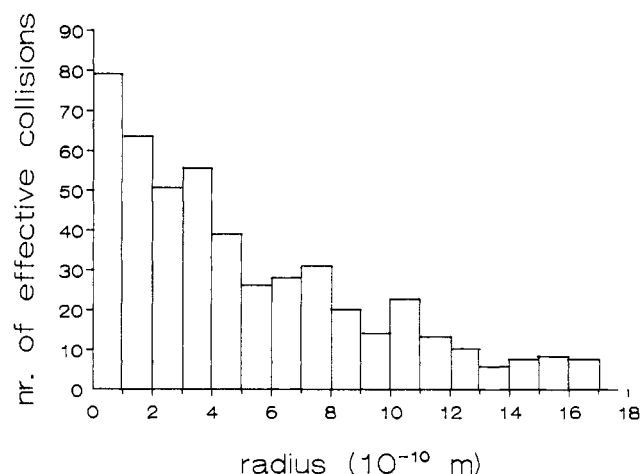


Figure 5. Result of the molecular dynamics calculation of the collision of He with two benzene molecules at 200 K. The horizontal axis shows the distance of closest approach of He to the center of the dimer. The vertical axis displays the number of effective collisions as a function of this distance.

and E_0 is the relative kinetic energy with which the two molecules approach each other. With the average energy $E_0 = k_B T$ for colliding systems, this yields for the energy-averaged collision time $\tau_{coll} = 1.5 \sigma \mu^{1/2} \epsilon^{1/6} (k_B T)^{-2/3}$.

We have carried out the molecular dynamics calculations of the collision of helium with two benzene monomers at three different temperatures: 200, 100, and 50 K. The parameters for the Lennard-Jones potential were taken from Sherwood and Prausnitz²¹ for benzene and from Hirschfelder et al.²² for helium. We chose 20 initial benzene dimer configurations and for each configuration 20 velocity vectors of He, and with these we carried out calculations with 50 different initial He positions. The calculations were carried out with a leapfrog algorithm.²³ A time step of 5 fs assured conservation of energy during the calculations. A He collision was called stabilizing if after the collision the total energy of the complex was smaller than the centrifugal barrier and the intradimer distance was less than r_{max} , the position of the centrifugal barrier. Figure 5 shows the number of effective collisions (out of 20 000) as a function of the distance of closest approach of the He to the center of the dimer. By taking the integral and dividing by 20 000, we find a value for the efficiency of a collision of $\eta = 0.024$. For 100 and 50 K we found $\eta = 0.020$ and 0.029 , respectively. Apparently, the efficiency does not strongly depend on temperature. We adopted the average value $\eta = 0.024$.

We can now insert this efficiency into eq 7 for the probability, taking for the He-benzene dimer the collision radius $(2^{1/3}\sigma_B + \sigma_{He})/2 = 6.7 \text{ \AA}$. Here we have assumed that the dimer is spherical and that the monomer volumes ($=4/3\pi\sigma^3$) are additive. We can evaluate this expression as a function of distance from the nozzle using the values of the He density as derived from the adiabatic expansion. We then arrive at the cooling probability as a function of distance from the nozzle with 1.5 atm of He pressure as given in Figure 6. Apparently, the rapid dilution of helium completely dominates the increase in lifetime with decreasing temperature.

Growth of Larger Clusters

The growth of larger clusters is considerably easier than the formation of a dimer, because now there are other van der Waals modes into which the van der Waals energy of condensation can be stored. But if the complex is not cooled by helium, it will eventually evaporate a monomer to lose its excess energy. The rate at which this occurs can be described in terms of RRK theory.⁸ For A addition we can write

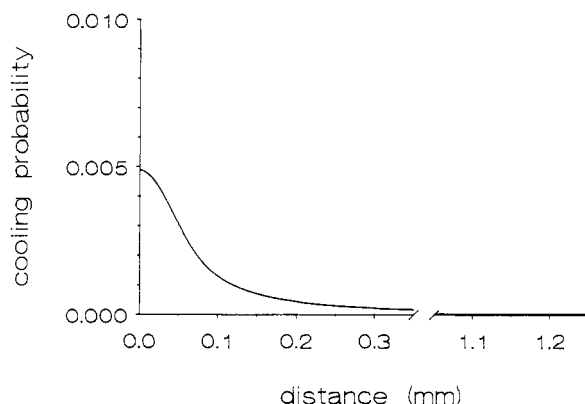


Figure 6. Theoretical probability that a monomer-monomer collision leads to dimer formation versus distance from the nozzle (100 μm). In the calculation we used a He pressure of 1.5 atm.

$$k_{\text{diss}}^A = \omega \frac{m}{m+n} \frac{(j+s-1)!/j!}{(j+p+s-1)!/(j+p)!}$$

$$k_{\text{sub}}^A = \omega \frac{n}{m+n} \frac{(j+p-q+s-1)!/(j+p-q)!}{(j+p+s-1)!/(j+p)!}$$

where s is the number of degrees of freedom ($=3(m+n)-6$), p is the number of quanta condensation energy of molecule A, q is the number of quanta condensation energy of molecule B, and j is the number of quanta in the complex before addition: $j = r(3(m+n-1)-5)$ for $m+n=3$ and $j = r(3(m+n-1)-6)$ for all other clusters, with r the average number of quanta per oscillator. In the above equations ω is a frequency factor, which usually has the order of magnitude of a van der Waals vibration frequency.

For B addition we have

$$k_{\text{diss}}^B = \omega \frac{n}{m+n} \frac{(j+s-1)!/j!}{(j+q+s-1)!/(j+q)!}$$

$$k_{\text{sub}}^B = \omega \frac{m}{m+n} \frac{(j+q-p+s-1)!/(j+q-p)!}{(j+q+s-1)!/(j+q)!}$$

We can calculate the number of quanta in the A-A well by taking the second derivative of the interaction potential $V(r)$ at equilibrium distance $r = r_e$. The resulting force constant k gives the harmonic frequency ω at the bottom of the well according to $\omega = (k/\mu)^{1/2}$, with μ the reduced mass. If ϵ is the well depth, then, in the harmonic approximation, the number of quanta in the well is taken to be $p = \epsilon/\hbar\omega$.

Results and Analysis

As a demonstration of the theory we developed for the formation kinetics of small weakly bound clusters, we studied two binary mixtures: benzene/toluene and toluene/*o*-xylene. This series was chosen because the interaction between the constituent cluster molecules increases from dipole-induced dipole in the first mixture to a somewhat stronger dipole-dipole interaction in the last mixture. All binary mixtures were measured with two or three concentrations of the constituents in the gas phase. Expansion conditions were such that there was a well-controlled constant gas flow during a time required to obtain sufficient statistics for all mass peaks. All mass peaks were integrated; the standard deviations for their relative intensities were approximately 5%.

Because the transmission of a quadrupole mass spectrometer is highly dependent on the mass range filtered and the ionizer lens settings, it is only valid to study the peak intensity distribution within a limited mass range, i.e., a certain cluster size. Because of the maximum spectrometer mass range, we limited ourselves to clusters up to the size of eight molecules. This has the advantage

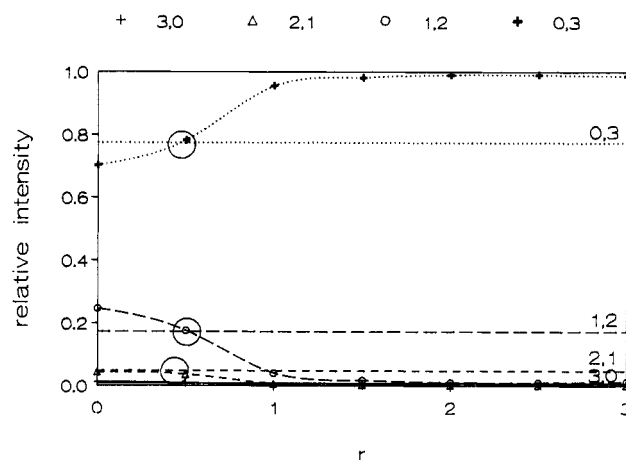


Figure 7. Comparison of theory and experiment for the trimer of a 70:30 benzene/toluene vapor mixture. Intensities are given relative to the sum of the trimer intensities. Experimental intensities are displayed by horizontal lines. The constitution of the clusters is given by the numbers just above these lines (2,1 corresponds to benzene₂/toluene₁). Calculated cluster intensities are plot as a function of r , the average number of quanta of vibrational energy present in the van der Waals wells before addition of another molecule. The efficiency of a helium collision is taken to be $\xi = 0.05$. The crossings of corresponding experimental and calculated intensities are indicated by circles. Note that r hardly depends on the constitution of the cluster.

that no shell formation takes place,²⁴ and by consequence we do not have to differentiate between bulk and surface molecules of the clusters. The latter effect would have made it necessary to modify our model, because with increasing cluster size the number of monomers would still increase linearly with size, but this would no longer be compensated by a linear increase of the number of dissociative molecules, because dissociation can only occur at the surface of the cluster. As a consequence, the substitution rate will decrease rapidly with increasing cluster size.

Having collected this large set of data, we fitted the theory to the experimental intensity distributions, using the dimer efficiency calculated above (see Figure 6) and the following parameters. From the work of Ernstberger et al.,⁴ we have for the benzene/benzene interaction 70 meV and for toluene/toluene, 150 meV. The first value is also obtained from fitting a Kihara potential to virial coefficients.²¹ From these latter data we obtain $\omega = 1.0 \times 10^{13} \text{ s}^{-1}$, the harmonic frequency in the harmonic van der Waals well. It then takes approximately 10 quanta to dissociate the benzene dimer: $p = 10$. Assuming the van der Waals frequency of the toluene/toluene dimer to be the same, it takes approximately 20 quanta to dissociate that dimer: $q = 20$. Seeing that the presence of a methyl dipole adds about 10 quanta to the interaction, we estimate that the presence of two methyl dipoles at an angle of 60° should add about 17 quanta to the interaction. For the *o*-xylene/*o*-xylene interaction we take $q = 27$. The values of p and q were taken to be independent of cluster size and cluster constitution. For the efficiency factor ξ we took values approximately equal to the value of η , the He dimer efficiency. The additional parameter r could only be varied within a limited range, the upper limit being set by the initial temperature of the expansion. This limit is approximately given by $r = 4$.

As an example, in Figures 7–9 we give a comparison of theory and experiment for the 3, 5, and 7 clusters of a 70:30 vapor mixture of benzene and toluene. We plot here the computer-predicted cluster intensities as a function of the average number of quanta per degree of freedom (r) for each cluster component and display in the same figure the experimental cluster intensities by horizontal lines. From the data it is clear that a good fit to the intensity distribution within one cluster size is obtained for a value of $r = 0.5$ and for a value of the helium efficiency of $\xi = 0.05$. As becomes apparent from the plots, the value of r is almost constant within one cluster distribution. This is a striking

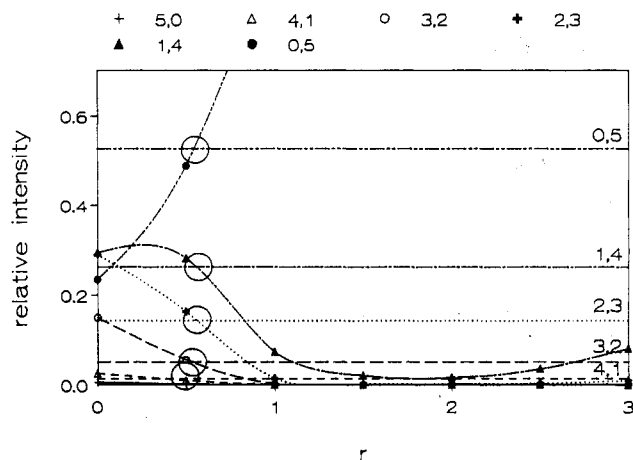


Figure 8. A plot as Figure 7, but now for the pentamer of a 70:30 vapor mixture of benzene/toluene.

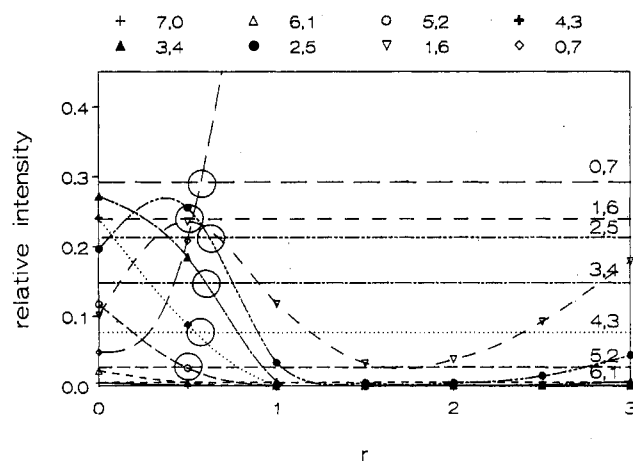


Figure 9. A plot as Figure 7, but now for the heptamer of a 70:30 vapor mixture of benzene/toluene.

result, since the slopes of the calculated curves are very steep and cluster distributions are very sensitive to small changes in the value of r . For the 90:10 vapor mixture of benzene/toluene we also found r to be independent of the cluster constitution within one cluster distribution. As could be expected, we found a slightly higher value of $r = 0.8$ at the same value of ξ , because in the latter composition the total vapor pressure is higher and therefore clusters experience on average fewer helium collisions between two successive monomer encounters. The calculations on the toluene/*o*-xylene mixture gave good agreement with experiment using the same helium efficiency as above of $\xi = 0.05$. For the 70:30 mixture we found a value of $r = 1.0$. Contrary to our expectations, we found for the 90:10 mixture a slightly lower value of $r = 0.8$. The reason why r is lower in the latter mixture is not clear to us. But since in both mixtures the values of r are close to one another, we do not speculate about it.

For both the benzene/toluene and the toluene/*o*-xylene mixture we obtain relatively small values for r compared to p and q , indicating that in each intermolecular potential well on average one or less than one level is occupied. This justifies our assumption that we can approximate the intermolecular well by a harmonic one to calculate values for p and q .

From Figures 7–9 it also becomes apparent that in cold clusters the enrichment will be very small. The reason for this is that in cold clusters ($r \approx 0$) the substitution reaction rate would be very small and that substitution would be completely dominated by

stabilization. The fact that we find values of r larger than zero indicates that clusters are still warm when they collide with a monomer. We can estimate that in the 70:30 mixture of benzene/toluene the average temperature of the clusters before addition of a monomer is 40 K. For the 90:10 mixture we estimate the temperature to be 60 K. For toluene/*o*-xylene we find temperatures of approximately 80 and 60 K for the 70:30 mixture and the 90:10 mixture, respectively. We want to emphasize that these are average temperatures, averaged over the region of the expansion. The real temperatures of the clusters will be higher near the nozzle exit but lower further downstream; i.e., clusters are really cold once they reach the collision-free zone. Then it is not necessary to include an extra step in the calculations which accounts for the decay of the clusters on their flight from the sudden freeze plane to the detector.

It is worth mentioning that we also studied the composition of mixed clusters of hexane and heptane. They are highly enriched on the heptane side, more so than would follow from a simple difference in the van der Waals interaction. At the present we are trying to find out what the cause is of this deviant behavior.

Acknowledgment. The support of Dr. E. Apol and Dr. J. G. E. M. Fraaije on the molecular dynamics calculations is gratefully acknowledged. J.K. acknowledges Joshua Jortner's suggestion a long time ago to start with supersonic beams. It certainly paid off!

References and Notes

- (1) Jonkman, H. T.; Even, U.; Kommandeur, J. *J. Phys. Chem.* **1985**, *89*, 4240.
- (2) Kiermeier, A.; Ernstberger, B.; Neusser, H. J.; Schlag, E. W. *J. Phys. Chem.* **1988**, *92*, 3785.
- (3) Booze, J. A.; Baer, T. *J. Chem. Phys.* **1993**, *98*, 186.
- (4) Ernstberger, B.; Krause, H.; Kiermeier, A.; Neusser, H. J. *J. Chem. Phys.* **1990**, *92*, 5285.
- (5) *Nucleation*, Zettlemoyer, A. C., Ed.; Marcel Dekker: New York, 1969.
- (6) Wilemski, G. *J. Chem. Phys.* **1984**, *80*, 1370.
- (7) Zeng, X. C.; Oxtoby, D. W. *J. Chem. Phys.* **1991**, *95*, 5940.
- (8) See for instance: Robinson, P. J.; Holbrook, K. A. *Unimolecular Reactions*; Wiley: New York, 1972.
- (9) Landolt-Börnstein. *Zahlenwerte und Funktionen*; 6. Auflage, 2. Teil, Bandteil a, Gleichgewichte Dampf-Kondensat und osmotische Phänomene; Springer: Berlin, 1960; pp 336–711.
- (10) *Handbook of Chemistry and Physics*, 67th ed.; CRC Press: Boca Raton, FL, 1986–1987.
- (11) Habets, A. H. M. Supersonic Expansion of Argon into Vacuum. Ph.D. Thesis, Technical University of Eindhoven, The Netherlands.
- (12) Miller, R. D. Free Jet Sources. In *Atomic and Molecular Beam Methods*; Scoles, G., Ed.; Oxford University Press: New York, 1988; pp 14–53.
- (13) Becker, E. W.; Bier, K.; Burghof, H. Z. *Naturforsch.* **1955**, *10A*, 565.
- (14) Sherman, F. S. *Phys. Fluids* **1965**, *8*, 773.
- (15) Rothe, D. E. *Phys. Fluids* **1966**, *9*, 1643.
- (16) Knuth, E. L. Direct-Sampling Studies of Combustion Processes. In *Engine Emission: Pollutant Formation and Measurement*; Springer, G. S., Patterson, D. J., Eds.; Plenum: New York, 1973; pp 319–363.
- (17) Sharma, P. K.; Knuth, E. L.; Young, W. S. *J. Chem. Phys.* **1976**, *64*, 4345.
- (18) Landolt-Börnstein. *Zahlenwerte und Funktionen*; 6. Auflage, 5. Teil, Bandteil b, Transportphänomene II, Kinetik homogene Gasgleichgewichte; Springer: Berlin, 1986; pp 204–218.
- (19) Feller, W. *An Introduction to Probability Theory and its Applications*, 3rd ed.; Wiley: New York, 1968; Vol. 1, pp 156–159.
- (20) Bunker, D. L. *J. Chem. Phys.* **1960**, *32*, 1001.
- (21) Sherwood, A. E.; Prausnitz, J. M. *J. Chem. Phys.* **1964**, *41*, 429.
- (22) Hirschfelder, J. O.; Curtiss, C. F.; Bird, R. B. *Molecular Theory of Gases and Liquids*; Wiley: New York, 1954.
- (23) Berendsen, H. J. C.; van Gunsteren, W. F. Practical Algorithms for Dynamic Simulations. In *Proceedings of the International School of Physics "Enrico Fermi", Molecular-Dynamics Simulation of Statistical-Mechanical Systems*; Cicciotti, G., Hoover, W. G., Eds.; North-Holland: Amsterdam, 1986; pp 43–65.
- (24) Easter, D. C.; Khoury, J. T.; Whetten, R. L. *J. Chem. Phys.* **1992**, *97*, 1675.